*Journal of Thermal Analysis and Calorimetry, Vol. 72 (2003) 631–640*

# INFLUENCE OF THE MOLECULAR MASS ON THE SEGMENTAL RELAXATION TIMES OF POLYSTYRENE DETERMINED BY DSC

*F. Hernández Sánchez*[1], *J. M. Meseguer Dueñas*[2*] *and*
*J. L. Gómez Ribelles*[2]

[1]Centro de Investigación Científica de Yucatán, C.43 No. 130 Chuburná de Hidalgo,
CP 97200 Mérida, México
[2]Centro de Biomateriales, Universidad Politécnica de Valencia, Camino de Vera s/n,
46071 Valencia, Spain

## Abstract

The segmental dynamics of narrow fractions ($\langle M_w \rangle / \langle M_n \rangle \approx 1.05$) of polystyrene with molecular masses ranging from 4000 to 600000 has been characterised by DSC. The samples were subjected to different thermal histories previously to the recorded heating scans including cooling from equilibrium at different cooling rates and annealing at different temperatures for different times. The fragility parameter $m=[\partial \log\tau / \partial (T_g/T)]_{T_g}$ was determined from the dependence of the glass transition temperature on the cooling rate from an equilibrium state. The curve that represents the enthalpy loss during the isothermal annealing *vs.* the annealing temperature for a fixed annealing time (180 min) shows a peak which can be used to describe the temperature interval in which the conformational rearrangements takes place at a rate compatible with the annealing time. This peak shifts towards higher temperatures when the molecular mass increases due to the shift of the glass transition temperature but the plot *vs.* $T_g/T$ is independent on the molecular mass. The β parameter of the stretched exponential and the temperature dependence of the relaxation time were calculated through modelling that confirms that the fragility of the polymer is independent of molecular mass.

**Keywords:** fragility, glass transition, molecular mass, polystyrene, structural relaxation

## Introduction

The key characteristic of the segmental dynamics of non-crystalline polymeric chains is its co-operative character. A conformational rearrangement involves a number of chain segments pertaining to different neighbouring chains. The volume element in which the rearrangement takes place without affecting the rest of the material is called a co-operative rearranging region [1]. A consequence of the co-operativity is the non-linear dependence of the logarithm of the relaxation times of the conformational rearrangements with the reciprocal of temperature. The temperature dependence of the relaxation times is non-Arrhenius and can be described by the empirical VFTH equation [2–4].

---

* Author for correspondence: E-mail: jmmesegu@fis.upv.es

*1388–6150/2003/ $ 20.00*

*Akadémiai Kiadó, Budapest*
*Kluwer Academic Publishers, Dordrecht*

$$\tau(T)=\tau_0\exp\frac{B}{T-T_0} \tag{1}$$

The conformational relaxation times can be measured using different experimental techniques. The viscoelastic response of the material (measured by means of creep, stress relaxation or dynamic-mechanical experiments) in the temperature region of the main or $\alpha$ relaxation is governed by the main-chain conformational rearrangements and the same occurs with the dielectric response in the main dielectric relaxation region. The glass transition and the structural relaxation process [5, 6], that can be characterised by volume or enthalpy measurements, are also a consequence of the temperature dependence of the conformational relaxation times.

In order to compare the relaxation times of different amorphous polymers it has been proposed to normalise the temperature axis with the glass transition temperature by plotting the values of $\log\tau$ *vs.* $T/T_g$, being $T_g$ the glass transition temperature defined in a more or less arbitrary form. This is the fragility plot proposed by Angell [7].

The comparison of the fragility plots of a series of polymers with the same chemical structure but varying $T_g$ is interesting as a test of the fragility schema. Roland and Ngai [8] analysing compliance data of Plazek and O'Rourke [9] concluded that there is no influence of the molecular mass on the fragility plot of polystyrene. Privalko *et al.* found [10], by DSC, a systematic dependence of the apparent activation energy at the glass transition $\Delta h^*$, being $\Delta h^*/R{=}\mathrm{d}\ln\tau/\mathrm{d}1/T_{T_g}$ and also a systematic dependence of the $\beta$ parameter of the stretched exponential or KWW equation

$$\phi(t)=\exp\left(-\frac{t}{\tau}\right)^{\beta} \tag{2}$$

that was used to characterize the shape of the relaxation function. A relationship has been proposed between the fragility and the $\beta$ parameter [11] in such a way that the results in [10] seems to point that there could be also an influence of the molecular mass on the fragility plot of polystyrene as determined by calorimetry.

In this work the structural relaxation process of four polystyrenes with varying molecular mass and narrow molecular mass distributions was studied by differential scanning calorimetry, DSC. The samples were subjected to a broad set of thermal histories with the aim to conclude if the kinetics of conformational rearrangements can be normalized using the fragility schema.

## Experimental

The samples used in this work were narrow fractions ($M_n/M_w\leq1.06$) of atactic polystyrene (Polysciences Inc.). The five samples with average molecular masses $M_w$=$4\cdot10^3$, $20\cdot10^3$, $200\cdot10^3$ and $600\cdot10^3$ will be designed PS4, PS20, PS200 and PS600, respectively.

A Perkin Elmer Pyris 1 DSC was used in all the experiments. All the thermal treatments were carried out in the calorimeter. Only one sample of each polymer, around 5 mg mass, sealed in an aluminium pan, was used for all the experiments.

All the experiments started at 412 K with the sample in equilibrium. In a series of experiments the sample was cooled at different cooling rates from 412 to 333 K (293 K in the case of PS4) and then heated at 10 K min$^{-1}$. The DSC curve measured on heating after cooling the sample at 40 K min$^{-1}$ will be called the reference scan. In other series of experiments the sample was cooled at 40 K min$^{-1}$ from 412 K to a temperature $T_a$, annealed at this temperature for a time $t_a$ and then cooled again at 40 K min$^{-1}$ to 333 K (293 K in the case of sample PS4). The heating scan followed at 10 K min$^{-1}$. Only the DSC curves recorded on heating will be analysed in this work.

## Results

The DSC curves measured on heating at 10 K min$^{-1}$ after cooling at different cooling rates $q_c$ can be used to determine the apparent activation energy $\Delta h^*$ using the relationship existing between the temperature dependence of the relaxation time and the dependence of $T_g$ on the cooling rate in the formation of glass [12]

$$\frac{\Delta h^*}{R}=\left.\frac{\mathrm{d}\ln\tau}{\mathrm{d}1/T}\right|_{T_g}=-\frac{\mathrm{d}\ln q_c}{\mathrm{d}1/T_{f'}} \tag{3}$$

where $T_{f'}$ is the fictive temperature in the glassy state reached after cooling which coincides with the glass transition temperature determined as the crossing point of the enthalpy lines corresponding to the equilibrium liquid and to the glass (the enthalpic glass transition temperature). As an example Fig. 1 shows the DSC curves measured for sample PS4 after cooling at rates ranging from 0.5 to 40 K min$^{-1}$. The height of the peak con-

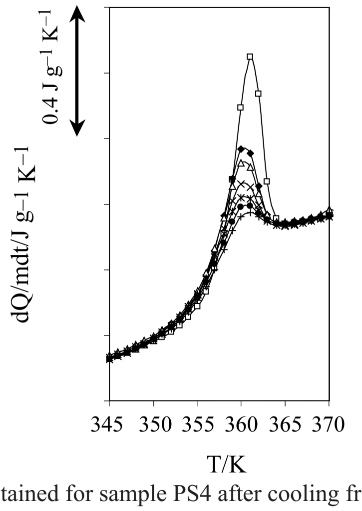

**Fig. 1** DSC curves obtained for sample PS4 after cooling from equilibrium at different cooling rates. □ – 0.5, ◆ – 2, △ – 3, × – 5, ∗ – 10, ● – 20 and + – 40°C min$^{-1}$

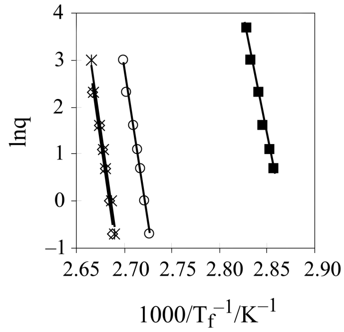

**Fig. 2** Fictive temperature attained in the glassy state $T_{f'}$ after cooling from equilibrium at different cooling rates $q_c$, represented in a ln$q_c$ *vs*. $1/T_{f'}$ plot

tinuously decreases as the cooling rate increases. It is noteworthy that the temperature of the maximum shown in the DSC curve first decreases as the cooling rate increases, goes through a minimum and then increases with further increases of the cooling rate, this behaviour seems to be general in chain polymers and has been described before [13, 14]. Figure 2 shows the plot of ln$q_c$ *vs*. the reciprocal of the glass transition temperature. The lines in Fig. 2 shift towards higher temperatures as the molecular mass increases (the glass transition temperature increases with the molecular mass) until sample PS200 as

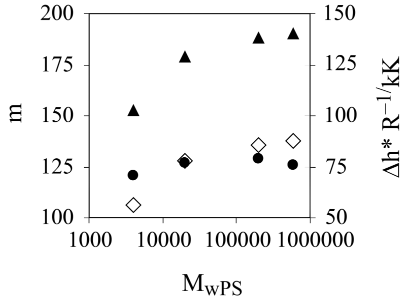

**Fig. 3** Apparent activation energy $\Delta h^*$ ▲ – at the glass transition temperature and the fragility parameter *m* ◇ – determined from results analogous to those shown in Fig. 2 for the samples with varying molecular mass. The values of the fragility parameter determined from the model parameters are ● – also shown

expected [15]. The glass transition temperature of samples PS200 and PS600 are equal within the experimental uncertainty. The value $\Delta h^*$ continuously increases with the molecular mass of the sample as shown in Fig. 3.

The influence of the annealing previous to the heating scan can be seen in the DSC curves shown in Fig. 4, where several DSC curves measured in PS4 sample are shown. The enthalpy loss during the isothermal stage, $\Delta h(T_a,t_a)$, which depends on the annealing temperature and time, was calculated from the DSC curves, $\Delta h(T_a,t_a)$ is equal to the area under the difference between the DSC curve measured after annealing and the reference scan (see for instance [16]). Figure 5 shows the values of $\Delta h(T_a,t_a)$ for all the samples annealed at different temperatures for 180 min. At high

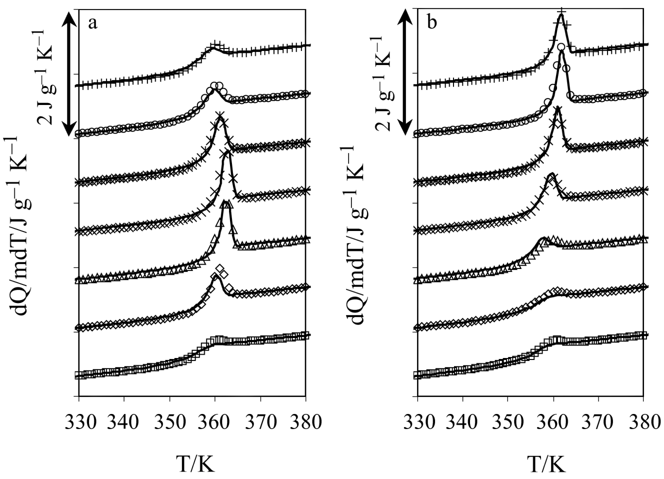

**Fig. 4** Normalised DSC curves obtained in sample PS4 after different thermal treatments a) □ – Reference scan, ◇ – annealing at 75°C for 30 min, △ – 720 min and × – 1440 min, cooling from equilibrium at ∗ – 0.5, o – 2 and + – 5°C min$^{-1}$. b) annealing for 180 min at □ – 45, ◇ – 50, △ – 55, × – 60, ∗ – 65, o – 70 and + – 75°C. The solid lines represent the model calculated curves using the parameters shown in Table 1

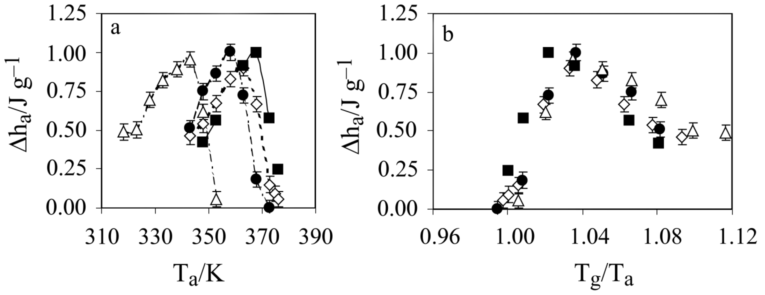

**Fig. 5** Enthalpy loss during the isothermal annealing for 180 min as a function of the a – annealing temperature and b – *vs.* ($T_g/T$). Sample ■ – PS600, ◇ – PS200, ● – PS20 and △ – PS4

temperatures, above the glass transition $\Delta h(T_a,t_a)=0$ because the sample is already in equilibrium at the beginning of the isothermal stage. As $T_a$ decreases the separation between the enthalpy when the annealing starts and that corresponding to equilibrium increases, so tending to increase the value of $\Delta h(T_a,t_a)$. But as $T_a$ decreases the rate of the structural relaxation process tending to approach equilibrium decreases. The opposite influence of these two factors explains the fact that, for a fixed value of the annealing time, $\Delta h(T_a,t_a)$ presents a maximum at a temperature which is around 10 degrees below the enthalpic glass transition temperature, as shown in Fig. 5.

## Discussion

The influence of the molecular mass on the conformational mobility can be analysed in terms of the fragility schema. On the one side the fragility parameter [17]

$$m=\left.\frac{\mathrm{dlog}\tau}{\mathrm{d}T_\mathrm{g}/T}\right|_{\mathrm{T_g}}=\frac{\Delta h^*}{2.303T_\mathrm{g}} \tag{4}$$

can be calculated from the results of Fig. 2. The result, as shown in Fig. 3, is that $m$ is an increasing function of the molecular mass, but with the exception of PS4 the values found for the other three samples are within the uncertainty of the determination of $m$ (the uncertainty in the calculation of $\Delta h^*$ can be around 20% [18]).

The kinetics of the structural relaxation process can be also analysed in terms of a fragility schema replotting $\Delta h(T_\mathrm{a},t_\mathrm{a})$ *vs.* $T_\mathrm{g}/T$ as shown in Fig. 5b. The curves merge in a single one within the accuracy of the experiments. The interval in which the conformational mobility is significant in the annealing for 180 min seems to be the same for the four samples.

The shape of the DSC curves recorded after different thermal histories contains information about the dynamics of the conformational rearrangements. Nevertheless the relationship between the experimental result and the temperature and structure dependence of the relaxation times is not easy due to the well known non-linearity and non-exponentiality of the process. The calculation of the relaxation times needs of the modelling of the relaxation process and the computer simulation of the experiments. This calculation includes, as a consequence, a series of assumptions that are still under discussion. In this work we will use the model proposed in [18] which has been applied with success to many polymer systems ([14, 18–23] and the references cited therein). The main equations of the model can be found in these references and only the main equations have been included in Appendix 1. The model assumes a shape of the relaxation function according to the stretched exponential of KWW equation, which includes a shape parameter $\beta$. The dependence of the average relaxation time with temperature and structure follows the Adam–Gibbs [1] relationship. The temperature dependence of the relaxation time in the equilibrium liquid follows an equation close to the VFTH equation, deduced from equations (A2) and (A4),

$$\tau^{\mathrm{eq}}(T)=A\exp\left(\frac{B}{T\int_{\mathrm{T_2}}^{\mathrm{T}}\frac{\Delta c_\mathrm{p}(T)}{T}\mathrm{d}T}\right) \tag{5}$$

The shape of this line is characterized by three parameters $A$, $B$ and $T_2$, the latter is the Gibbs–DiMarzio temperature [24] at which the configurational entropy in equilibrium vanishes.

The model assumes that the polymer in a glassy state kept in isothermal conditions, at temperature $T_\mathrm{a}$, is not able to evolve until the equilibrium state corresponding to the temperature $T_a$. Before that a metastable state is attained in which the configurational entropy is higher than in equilibrium but the chain packing is so high that the conformational mobility collapses. Thus, the limit state of the isothermal relaxation process is a value of entropy $S_c^{\lim}(T_a)$ rather than the equilibrium value $S_c^{\text{eq}}(T_a)$. It has been shown that in many polymers the introduction of this assumption in the model equations allows to reproduce accurately a broad set of DSC curves measured after different thermal histories with a single set of model parameters. The difference between $S_c^{\lim}(T_a)$ and $S_c^{\text{eq}}(T_a)$ is characterised by means of an additional parameter δ defined as shown in Fig. 7.

The set of parameters was determined by simultaneous least squares fit to a series of eight experimental DSC curves. Due to the strong correlation between the parameters $B$, $T_2$ and $A$, the parameter $B$ was kept constant in the search routine with a value of 1000 J $g^{-1}$ which was determined for polystyrene in [17]. The uncertainty in the calculation of the model parameters was determined following the procedure proposed in [25]. The values of the parameters were the average of the results obtained in the fit of ten sets of eight DSC curves randomly selected. The standard deviation was assumed to be the uncertainty of each parameter.

As a representative example of the results of computer simulation of the experiments, Fig. 4 shows the model calculated DSC curves (with the parameters shown in Table 1) corresponding to fourteen different thermal histories to which PS4 sample was subjected. Clearly the model equation are able to reproduce the experimental results with a single set of parameters, independent of the thermal history of the experiment. Thus the set of parameters obtained in this way is a good characterisation of the dynamics of the conformational rearrangements of the chain segments.

**Table 1** Sets of model parameters, obtained by curve fitting with B=1000 J $g^{-1}$, see text

| | δ | β | $T_2$/K | –ln$A$ | $T_g$/K | $T_g$–$T_2$/K |
|---|---|---|---|---|---|---|
| PS4 | 0.063±0.009 | 0.48±0.004 | 285.5±1.1 | –49.6±0.8 | 354.0 | 68.5 |
| PS20 | 0.061±0.009 | 0.49±0.004 | 303.5±1.1 | –43.5±0.8 | 371.3 | 67.8 |
| PS200 | 0.067±0.014 | 0.48±0.020 | 308.4±1.6 | –43.5±1.0 | 376.0 | 67.6 |
| PS600 | 0.051±0.010 | 0.46±0.009 | 303.1±1.0 | –47.1±0.7 | 376.3 | 73.2 |

In particular, the values of the parameters $A$, $B$ and $T_2$ (Table 1) allow to calculate, using Eq. (5), the temperature dependence of the relaxation times in equilibrium. As shown in Fig. 6, the relaxation times of the samples with different molecular masses fall on a single line in the fragility diagram. From these curves the fragility parameter $m$ can be also calculated. As shown in Fig. 3 the magnitude of $m$ agrees with the values calculated from the cooling rate dependence of the glass transition temperature, with the exception of the sample PS4. The differences between the values found for the different samples, in particular the fact that the value obtained for PS4 be smaller than in the rest of samples fall within the uncertainty of the calculation. Modelling of the experimental DSC curves yields a fragility independent on the

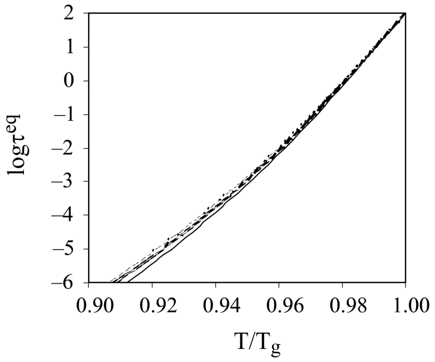

**Fig. 6** Temperature dependence of the equilibrium relaxation times, $\tau^{eq}(T)$, calculated for ----- – PS600, –··–··– – PS200, –·–·– – PS20 and – – – – PS4 with the sets of parameters of Table 1

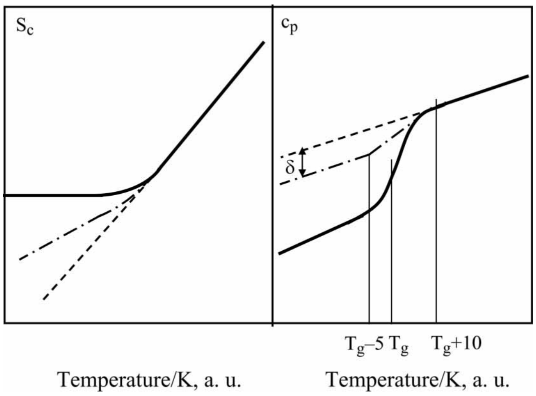

**Fig. 7** Sketch of the temperature dependence of configurational entropy (a) and heat capacity corresponding to the liquid state (dashed line), to an experimental cooling scan at a finite cooling rate (solid line), and to the hypothetical line of the limit states of the structural relaxation process (dashed-dotted line)

molecular mass. This result agrees with the mechanical results of Roland and Ngai [8].

We found no systematic dependence of the β parameter with molecular mass, in contrast with the result reported in [10]. The possible connection between the shape of the relaxation function and the fragility of the material [11], makes consistent that no significant change is found in β if no change was detected in the fragility parameter.

## Conclusions

The change of the molecular mass of polystyrene produces great changes in the dynamics of the co-operative conformational rearrangements of the chain segments due to the change in the concentration of end-groups. Nevertheless, the changes in the absolute values of the relaxation times, and, as a consequence the change in the glass transition temperature, does not implies a change in the fragility of the material or in the shape of the relaxation function. It is possible to normalise the results of the segmental dynamics of a series of samples that differ only in the molecular mass following the fragility schema.

## Appendix

The evolution of the configurational entropy during a thermal history that consists of a series of temperature jumps from $T_{i-1}$ to $T_i$ at time instants $t_i$, followed by isothermal stages is given by:

$$S_c(t)=S_c^{\lim}(T(t))-\sum_{i=1}^{n}\left(\int_{T_{i-1}}^{T_i}\frac{\Delta c_p^{\lim}(T)}{T}\mathrm{d}T\right)\exp\left[-\left(\int_0^t\frac{\mathrm{d}t'}{\tau(t')}-\int_0^{t_{i-1}}\frac{\mathrm{d}t'}{\tau(t')}\right)^{\beta}\right] \quad \text{(A1)}$$

The function $\tau(t)$ is determined implicitly by the dependence of $\tau$ on $T$ and $S_c$ during the thermal history, a dependence which is assumed to obey the equation of Adam and Gibbs [1] extended to non-equilibrium states:

$$\tau(T,S_c)=A\exp\left(\frac{B}{TS_c(t,T)}\right) \quad \text{(A2)}$$

$S_c^{\lim}(T)$ represents the value of the configurational entropy attained in the physical ageing process at infinite time, and $\Delta c_p^{\lim}(T)$ is defined through

$$S_c^{\lim}(T)=S_c^{eq}(T^*)+\int_{T^*}^{T}\frac{\Delta c_p^{\lim}(T)}{T}\mathrm{d}T \quad \text{(A3)}$$

with $T^*$ a temperature high enough above the glass transition and

$$S_c^{eq}(T)=\int_{T_2}^{T}\frac{\Delta c_p(T)}{T}\mathrm{d}T \quad \text{(A4)}$$

where $\Delta c_p(T)$ is the conformational heat capacity, here taken as the difference between the heat capacities of the liquid and the glass, $\Delta c_p(T)=c_{pl}(T)-c_{pg}(T)$ (a linear dependence of $\Delta c_p(T)$ with temperature has been assumed in this work) and $T_2$ is the Gibbs–DiMarzio temperature [24].

The phenomenological models of the structural relaxation usually assume that the state attained at infinite time in the structural relaxation process at a temperature $T_a$ can be identified with the extrapolation to $T_a$ of the equilibrium line experimentally determined at temperatures above $T_g$. When the models are based on the fictive temperature concept $T_f$ this is simply a result of the identification of the limit of $T_f$ at infinite time with $T$. In the context of our model this means that:

$$S_c^{\lim}(T)=S_c^{eq}(T)$$

However, it has been shown that the agreement between the model simulation and the experiments is highly improved when the model includes an assumption leading to values of $S_c^{\mathrm{lim}}(T)$ significantly higher than those of $S_c^{\mathrm{eq}}(T)$ [14, 19–23]. The definition of the curve $S_c^{\mathrm{lim}}(T)$ introduces new adjustable parameters in the model. The shape shown in Fig. 7 has been chosen because it needs only one additional parameter δ, defined as shown in the Fig 7.

* * *

This work was supported by the Spanish Ministerio de Educación y Ciencia DGICyT through the MAT 2000-0123-P4-03 project.

## References

1 G. Adam and J. H. Gibbs, J. Chem. Phys., 43 (1965) 139.
2 H. Vogel, Phys. Z., 22 (1921) 645.
3 G. A. Fulcher, J. Am. Ceram. Soc., 8 (1925) 339.
4 G. Tamman and W. Hesse, Z. Anorg. Allg. Chem., 156 (1926) 245.
5 R. O. Davies and G. O. Jones, Adv. Phys., 2 (1953) 370.
6 I. M. Hodge, J. Non-Cryst. Solids, 211 (1994) 169.
7 C. A. Angell, J. Non-Cryst. Solids, 131 (1991) 3.
8 C. M. Roland and K. L. Ngai, Macromolecules, 25 (1992) 5765.
9 D. J. Plazek and V. M. O'Rourke, J. Polym. Sci. Polym. Phys. Ed., 9 (1971) 209.
10 V. P. Privalko, S. Demchenko and Y. S. Lipatov, Macromolecules, 19 (1986) 901.
11 D. J. Plazek and K. L. Ngai, Macromolecules, 2 (1991) 1222.
12 C. T. Mohynihan, A. J. Easteal, M. A. DeBolt and J. Tucker, J. Amer. Ceram. Soc., 59 (1976) 12.
13 J. M. Hutchinson, S. Smith, B. Horne and G. M. Gourlay, Macromolecules, 32 (1999) 5046.
14 J. M. Meseguer Dueñas, A Vidaurre Garayo, F. J. Romero Colomer, J. Más Estellés, J. L. Gomez Ribelles and M. Monleón Pradas, J. Polym. Sci., Polym. Phys. Ed., 35 (1997) 2201.
15 J. M. G. Cowie Polymers: Chemistry and Physics of Modern Materials Blackie Academic & Professional, London 1973.
16 J. L. Gómez Ribelles, A. Ribes Greus and R. Díaz Calleja, Polymer, 31 (1990) 223.
17 R. Böhmer, K. L. Ngai, C. A. Angell and D. J. Plazec, J. Chem. Phys., 99 (1993) 418.
18 I. M. Hodge and J. M. O'Reilly, J. Phys. Chem. B, 103 (1999) 4171.
19 J. L. Gómez Ribelles and M. Monleón Pradas, Macromolecules, 28 (1995) 5867.
20 A. Brunacci, J. M. G. Cowie, R. Ferguson, J. L. Gómez Ribelles and A. Vidaurre Garayo, Macromolecules, 29 (1996) 7976.
21 J. L. Gomez Ribelles, M. Monleon Pradas, A. Vidaurre Garayo, F. Romero Colomer, J. Más Estelles and J. M. Meseguer Dueñas, Polymer, 38 (1997) 963.
22 J. L. Gómez Ribelles, A. Vidaurre Garayo, J. M. G. Cowie, R. Ferguson, S. Harris and I. J. McEwen, Polymer, 40 (1998) 183.
23 C. Torregrosa, A. Vidaurre, J. M. Meseguer Dueñas, M. Salmerón, M. Monleón Pradas and J. L. Gómez Ribelles, Colloid Polym. Sci., 277 (1999) 1033.
24 J. H. Gibbs and E. A. DiMarzio, J. Chem. Phys., 28 (1958) 373.
25 A. Saiter, J. M. Oliver, J. M. Saiter and J. L. Gómez Ribelles, submitted.